HHS Public Access

Author manuscript

*Cancer Gene Ther*. Author manuscript; available in PMC 2015 January 01.

Published in final edited form as:

*Cancer Gene Ther*. 2014 July ; 21(7): 264–274. doi:10.1038/cgt.2014.26.

# Experimental virotherapy of chemoresistant pancreatic carcinoma using infectivity-enhanced fiber-mosaic oncolytic adenovirus

**Sergey A. Kaliberov**[1], **Lyudmila N. Kaliberova**[1], **Donald J. Buchsbaum**[2], and **David T. Curiel**[1]

[1]Department of Radiation Oncology, School of Medicine, Washington University in St. Louis, St. Louis, Missouri, United States of America

[2]Division of Radiation Biology, Department of Radiation Oncology, University of Alabama at Birmingham, Birmingham, Alabama, United States of America

## Abstract

Pancreatic cancer is a significant clinical problem and novel therapeutic approaches are desperately needed. Recent advances in conditionally replicative adenovirus-based (CRAd) oncolytic virus design allow the application of CRAd vectors as a therapeutic strategy to efficiently target and eradicate chemoresistant pancreatic cancer cells thereby improving the efficacy of pancreatic cancer treatment. The goal of this study was to construct and validate the efficacy of an infectivity-enhanced, liver-untargeted, tumor-specific CRAd vector. A panel of CRAds has been derived which embody the C-X-C chemokine receptor type 4 promoter for conditional replication, two fiber complex mosaicism for targeting expansion, and hexon hypervariable region 7 (HVR7) modification for liver untargeting. We evaluated CRAds for cancer virotherapy using a human pancreatic tumor xenograft model. Employment of the fiber mosaic approach improved CRAd replication in pancreatic tumor xenografts. Substitution of the HVR7 of the Ad5 hexon for Ad serotype 3 hexon resulted in decreased liver tropism of systemically administrated CRAd. Obtained data demonstrated that employment of complex mosaicism increased efficacy of the combination of oncolytic virotherapy with chemotherapy in a human pancreatic tumor xenograft model.

### Keywords

targeted oncolytic adenovirus; pancreatic cancer; gemcitabine; fiber; hexon

## INTRODUCTION

Pancreatic cancer is one of the most aggressive types of malignancies. In this regard, pancreas adenocarcinomas account for the majority of all pancreas cancers and have a



CONFLICT OF INTEREST

The authors declare no conflict of interest.

dismal five-year survival rate of 6% [1]. The existing treatment options for pancreatic cancer have all thus far fallen short of breakthrough success [2]. While the introduction of gemcitabine slightly improved the one-year survival rate, it has only a 5.4% partial response rate and imparts a progression-free survival interval ranging from 1.9 to 4.3 months [3]. The reason for this poor response is believed to be dependent on a subset of cancer cells exhibiting chemotherapy resistance [4]. Apart from gemcitabine (plus erlotinib), FOLFIRINOX, a combination of 5-fluorouracil, irinotecan and oxaliplatin [5] as well as gemcitabine plus nanoparticle albumin-bound nab-paclitaxel [6] are novel therapeutic options for patients with metastatic pancreatic ductal adenocarcinoma. These data clearly indicate that it is imperative to exploit new therapeutic approaches to improve the clinical outcome of this disease. Thus, development of an effective therapy for the treatment of advanced pancreatic cancer is predicated on efficiently targeting and eradicating chemoresistant tumor cells.

A growing body of evidence demonstrates the promise of gene therapy and oncolytic virotherapy in preclinical and early clinical studies. Oncolytic viruses are a targeted therapy based on the cytolytic effect of replicating viruses. Among them adenovirus (Ad)-based systems have unique advantages for targeting pancreatic cancers. Unlike other oncolytic viruses, Ad does not require active cell proliferation for its replication. Stringent Ad replication specificity can be achieved by placing viral genes necessary for replication under the control of tumor-specific promoters, thereby generating conditionally replicative adenoviruses (CRAds) [7]. However, CRAds based on the conventional Ad vector structure demonstrated limited clinical efficacy [8].

Thus, despite the conceptual promise embodied in developed CRAd agents, design advancements are presently required. Of note in this regard, targeting must embody the concept that tumors are complex tissues which are composed of many interdependent cellular components, including malignant cells and tumor-associated stromal elements. Pancreatic cancer offers one of the most striking examples of such heterogeneity: 1) carcinomas of the pancreas are characterized by an intense desmoplastic response which consists of an altered extracellular matrix with microvascular hyperplasia, and involved inflammatory cells and stromal fibroblasts, as the paramount feature of their phenotype [2]; 2) over the past decade, evidence has demonstrated that the capacity of a tumor to grow and propagate is dependent on a small subset of cells, recently identified as pancreatic cancer stem (or stem-like) cells (CSCs) [9–11]. Due to their vital role in tumor maintenance and the formation of the resistance to current therapies, CSCs are integral targets to treat pancreatic cancer, as current therapeutic regimens cannot effectively treat this cell population because of its intrinsically resistant nature [12].

In this regard, the goal of the work reported here was to design, develop and characterize a clinically relevant virotherapy agent for carcinoma of the pancreas. A central facet of our approach is to confer the CRAd capacity to infect a diversity of pancreatic cancer tumor cells and tumor-associated targets. To this end we have developed mosaic CRAd vectors with fibers derived from both Ad serotype 5 and serotype 3. This fiber profile allows the expanded tropism required for an “inclusion targeting” strategy – viral particles which can efficiently infect tumor cells with a distinctive receptor’s repertoire. In addition, in order to

confer the CRAd replication specificity to pancreatic cancer cells, we have employed the promoter element of the C-X-C chemokine receptor type 4 (CXCR4) gene. We evaluated CRAd vectors which employ tropism expansion for inclusion targeting and hexon modifications for liver untargeting for oncolytic virotherapy using a human pancreatic tumor xenograft model. Obtained data demonstrated that employment of fiber from Ad serotype 3 increased CRAd replication in chemotherapy resistant pancreatic tumor xenografts. Substitution of the hypervariable region 7 (HVR7) of the Ad5 hexon for the Ad serotype 3 hexon resulted in decreased liver tropism of systemically administrated CRAd vector. An experimental therapy study using a human pancreatic tumor xenograft model demonstrated that employment of complex mosaicism increased efficacy of the combination of oncolytic virotherapy with chemotherapy. These findings highlight the improved antitumor activities that may accrue with advancements in the design of CRAd agents for cancer of the pancreas.

## MATERIALS AND METHODS

### Cells and reagents

MiaPaCa-2 and BxPC-3 human pancreatic cancer cells were obtained from American Type Culture Collection (Manassas, VA). The Chinese hamster ovary CHO cells, CHO-CAR cells expressing hCAR and CHO-C2 cells expressing CD46 were provided by Dr. H. Ugai (Washington University in St. Louis, St. Louis, MO). HEK293 human embryonic kidney cells were purchased from Microbix Biosystems Inc. (Ontario, Canada). L3.6, AsPC-1, HS7665, Capan-1 and HPAF-II human pancreatic cancer cells were kindly provided by Dr. P. Oliver (University of Alabama at Birmingham, Birmingham, AL). All cells were cultured in DMEM/F12 (Mediatech, Herndon, VA) containing 10% fetal bovine serum (FBS) (Summit Biotechnology, Fort Collins, CO). Panc2.03 human pancreatic cancer cells (a kind gift from Dr. E. Jaffee, Johns Hopkins University, Baltimore, MD) were cultured in RPMI-1640 containing 1.0 mM sodium pyruvate, 0.1 mM non-essential amino acids, 0.01 mg/ml bovine insulin (Mediatech) and 10% FBS (Summit Biotechnology). All cells were cultured at 37°C in a 5% CO2 atmosphere without antibiotics. To establish chemotherapy resistant Capan-1G, L3.6G and AsPC- 1G cell lines, pancreatic cancer cells were plated into 6-well tissue culture plates at $2 \times 10^5$ cells per well, and allowed to adhere overnight. Next day, serial dilutions (50–1600 nM) of gemcitabine hydrochloride were added directly to cells. To grow a sufficient number of cells for culture expansion of stable clones, cells were incubated for 4 – 6 weeks.

Gemcitabine hydrochloride was purchased from Sigma-Aldrich (St. Louis, MO). Molecular cloning enzymes were purchased from New England Biolabs (Ipswich, MA).

### Adenoviral vectors

CRAd vectors were constructed using standard molecular cloning methods. Briefly, polymerase chain reaction (PCR) was employed to generate a PCR product encoding a fragment of the *E1* gene (nucleotides 560–3533). The PCR product was cloned into the pShuttle plasmid (Quantum Biotechnologies, Montreal, Canada) using *Xho* I and *Sal* I sites to generate the pShuttleE1. To develop the pShuttle-cxcr4-E1 plasmid encoding the *E1a* gene under control of the cxcr4 promoter, the fragment including the cxcr4 promoter

element was replaced from pShuttle-cxcr4-Luc plasmid [13] using *Hind* III site, blunted using DNA Polymerase I Klenow fragment and then digested using *Sal* I restriction endonuclease, and ligated with *Xho* I, blunted using DNA Polymerase I Klenow fragment and *Sal* I digested pShuttleE1 plasmid. The DNA inserts were confirmed by using restriction enzyme mapping and partial sequencing analysis.

Recombinant Ad genomes were generated by homologous DNA recombination in *Escherichia coli* BJ5183 between pShuttle-cxcr4-E1 and pAdEasy-1 plasmid (Quantum Biotechnologies) to generate pCRAdcxcr4H5-F5, or Ad5 fiber gene deleted pVK500C plasmid (kindly provided by Dr. V. Krasnykh, M. D. Anderson Cancer Center, Houston, TX) to generate pVK500C-cxcr4-E1 plasmid. pCRAdcxcr4H5-F3 and pCRAdcxcr4H5-F5/F3 vector genomes were generated by homologous DNA recombination in *Escherichia coli* BJ5183 between pVK500C-cxcr4-E1 and *BstA* I and *Kpn* I digested pKAN5T3SK or pKAN3.1F5cmv5T3 plasmids (kindly provided by Dr. H. Ugai, Washington University in St. Louis, St. Louis, MO), containing a gene encoding fiber Ad serotype 3 gene or a gene encoding wild-type fiber Ad serotype 5 gene and fiber Ad serotype 3 gene under control of the human cytomegalovirus (CMV) major immediate-early enhancer/promoter element, respectively. To generate hexon-modified pCRAdcxcr4H5/3-F5/F3, the *SexA* I - *Hpa* I digest product of Ad5 hexon was substituted with a 618 bp fragment from Ad serotype 3 hexon (nucleotides 1127–1745).

The newly generated genomes were confirmed by partial sequencing analysis, linearized with *Pac* I and transected into HEK293 cells using the SuperFect Transfection Reagent (Qiagen, Chatsworth, CA) to generate CRAdcxcr4H5-F5, CRAdcxcr4H5-F3, CRAdcxcr4H5-F5/F3 and CRAdcxcr4H5/3-F5/F3 recombinant Ads. Replication incompetent *E1*- and *E3*-deleted AdcmvLuc (encoding firefly luciferase (*Luc*) gene under control of the CMV promoter) and Adcxcr4Luc (encoding *Luc* under control of the cxcr4 promoter) vectors have been described previously [13]. All viruses were propagated in HEK293 cells, purified by cesium chloride gradient ultracentrifugation, and subjected to dialysis as previously described [14]. The concentration of viral particles (vp) was determined by measuring absorbance of the dissociated virus at A260 nm using a conversion factor of $1.1 \times 10^{12}$ vp per absorbance unit. Multiplicity of infection for subsequent experiments was expressed as vp per cell.

## Luciferase assay

Cells were seeded at $5 \times 10^4$ cells per well in 24-well tissue culture plates and allowed to grow overnight. The next day, cells were washed one time with PBS, and then infected with $1 \times 10^3$ vp per cell of Adcxcr4Luc or AdcmvLuc vectors in triplicate. After one hour, cell culture media was removed, the wells were washed with PBS and fresh media was added. After 48 hours, cell culture media was removed, and cells were washed one time with PBS, and lysed. The Luciferase Assay System (Promega, Madison, WI) and ORION microplate luminometer (Berthold Detection Systems, Oak Ridge, TN) were used for the evaluation of Luc activity of infected cells. Luciferase activity was normalized by the protein concentration of the cell lysate using DC Protein Assay (Bio-Rad, Hercules, CA), according

to the manufacturer's instructions. Data are expressed as relative light units (RLU) per $1 \times 10^4$ cells and bars represent the mean + the standard deviation (s.d.).

### *In vitro* cytotoxicity assay using crystal violet staining

To measure the cytotoxicity of gemcitabine, pancreatic cancer cells were plated into 96-well tissue culture plates at $5 \times 10^3$ cells per well, and allowed to adhere overnight. Next day, serial dilutions of gemcitabine were added directly to cells. Cells were incubated for 5 days, and relative cell density was determined using a crystal violet staining assay. Cell culture medium was removed and surviving cells were then fixed and stained with 2% (w/v) crystal violet (Sigma-Aldrich) in 70% ethanol for 3 hours at room temperature. The plates were extensively washed, air-dried and optical density was measured at 595 nm using an EL 800 Universal Microplate Reader (BIO-TEK Instruments, Winooski, VT). Fractional cell survival at each drug concentration was calculated as the ratio of absorbance at 595 nm of cells incubated in the presence *versus* absence of drug, corrected for background absorbance of media alone. Fractional cell survival data were plotted against drug concentration and the half maximal inhibitory concentration (IC50) values extrapolated by piecewise linear regression as the concentration of drug producing a 50% reduction in corrected absorbance.

### Animal studies

Animal studies were carried out in strict accordance with the recommendations in the Guide for the Care and Use of Laboratory Animals of the National Institutes of Health. All animals were housed under pathogen-free conditions according to the guidelines of the American Association for Accreditation of Laboratory Animal Care, with access to chow and water *ad libitum*. Female athymic nude mice 5–7 weeks old were purchased from the National Cancer Institute Frederick Cancer Research and Development Center (Frederick, MD). To assess therapeutic effects of gemcitabine on established solid tumors, AsPC-1 or AsPC-1G cells were mixed 2:1 (v/v) with Matrigel (Collaborative Biomedical Products, Bedford, MA), and $5 \times 10^6$ cells were injected subcutaneously (s.c.) into athymic nude mice. Treatment was started 10 days post-tumor cell injection at the time of established tumor growth (tumors were 6–8 mm in diameter), noted as Day 0. Mice were injected intraperitoneally (*i.p.*) with gemcitabine at 50 mg/kg or PBS on Days 0, 3, 5, and 7. Tumor size was monitored twice a week with digital Vernier calipers. Tumor volumes were calculated as $0.5 \times \text{length} \times \text{width}^2$ ($\text{mm}^3$) and plotted as a percentage change over time relative to the mean size on Day 0 for each group. Mean time to tumor doubling of the group receiving different treatments was calculated.

### Polymerase chain reaction (PCR)

To confirm the presence of chimeric fiber genes in the CRAd genomes, viral genomic DNA was extracted from $1 \times 10^7$ vp of purified viral stock by using a QIAamp DNA Mini Kit (Qiagen). For detection of the Ad fiber gene, the following primers were used: F-100 (nucleotides 30948-30969): 5'-CCT CCT GGC TGC AAA CTT TCT C-3' and F+100 (nucleotides 32945-32924): 5'-GAG GTG GCA GGT TGA ATA CTA G-3'. After the initial denaturation (5 min at 95°C), amplification was performed with 30 cycles of 15 sec at

92°C, 60 sec at 55°C and 60 sec at 72°C, final extension of 10 min at 72°C. PCR products were analyzed by 1% agarose electrophoresis with ethidium bromide staining.

### Western blotting

Samples were preincubated in Laemmli sample buffer at 99°C for 10 min and separated using a 4–20% gradient polyacrylamide Precise Protein gel (Thermo Scientific, Rockford, IL). For electrophoresis under semi-native condition, samples were not boiled. The proteins were electroblotted onto polyvinylidene difluoride (PVDF) membranes and the blots were developed with SIGMA FAST 3,3'-diaminobenzidine system (Sigma-Aldrich) according to the manufacturer's protocol using anti-Ad5 fiber tail mAb (4D2, NeoMarkers, Fremont, CA) and goat anti-mouse Ig-HRP (DakoCytomation Denmark A/S, Glostrup, Denmark) for Ad fiber protein detection.

### *In vitro* CRAd mediated cytotoxicity assay

To determine cell growth after CRAd infection, cells were seeded into 96-well tissue culture plates at $5 \times 10^3$ cells per well, incubated for 24 hours, and infected with CRAd vectors at $1 \times 10^3$ vp per cell. Ninety-six hours afterward, cell culture medium was removed and surviving cells were then fixed and stained with crystal violet as described above. Relative density of adherent cells was defined as OD595 treated cells in comparison with untreated cells and the OD595 value of blank wells was subtracted.

### Thermostability *in vitro*

Capan-1 cells were plated in 96-well tissue culture plates at a density of $5 \times 10^4$ cells per well, allowed to adhere and grow overnight. The next day, recombinant CRAds were preincubated at 45°C for different times then added to cells as described above. Ninety-six hours afterward, cell culture medium was removed and surviving cells were then fixed and stained with crystal violet as described above. Relative density of adherent cells was obtained by changing the OD595 readings of cells infected with the heat-treated viruses to the percentage of the readings of untreated viruses and the OD595 value of blank wells was subtracted.

### Expression of recombinant Ad5 and Ad3 knob

The knob domain of Ad5 and Ad3 fiber proteins were expressed in *Escherichia coli* as described previously [15]. Soluble His-tagged Ad5 and Ad3 fiber knob proteins were purified by gravity-flow affinity chromatography using a Ni-NTA resin (Qiagen). The concentration of the purified protein was determined using DC Protein Assay (Bio-Rad), according to the manufacturer's instructions. Purified recombinant proteins were evaluated by Western blot using anti-His mAb (Sigma-Aldrich).

### Competitive inhibition of CRAd infection

AsPC-1G cells were seeded at $5 \times 10^3$ cells per well in 96-well tissue culture plates and allowed to grow overnight. The next day, cells were incubated for one hour at 4°C with 100 mg/ml of Ad5 or Ad3 fiber knob proteins or bovine serum albumin (BSA). After incubation, cells were infected with $1 \times 10^3$ vp per cell of CRAdcxcr4H5-F5, CRAdcxcr4H5-F3,

CRAdcxcr4H5-F5/F3 for one hour at 37°C. Subsequently, cell culture media was removed, cells were washed with PBS, and fresh media was added. Cells were incubated for 5 days, and cytopathic effect of CRAd infection was determined using a crystal violet staining assay as described above.

## Real-time quantitative PCR

Quantitative analysis of the Ad5 hexon gene expression was performed using real-time PCR. For *in vitro* studies, CHO, CHO-CAR and CHO-C2 cells were plated into 6-well tissue culture plates at $3 \times 10^5$ cells per well, and allowed to adhere overnight. Next day, cells were infected with $1 \times 10^3$ vp per cell of CRAdcxcr4H5-F5, CRAdcxcr4H5-F3 or CRAdcxcr4H5-F5/F3. After incubation for one hour at 37°C cell culture media was removed, cells were washed one time with PBS, collected, and total DNA was extracted using QIAamp DNA Mini Kit (Qiagen). For preparation of control samples, CRAdcxcr4H5-F5 genomic DNA was extracted from purified viral stock by using a QIAamp DNA Mini Kit. Serial 10-fold dilutions (from $1 \times 10^9$ to 10 viral particles per reaction) of viral DNA were included in each run to establish a standard curve for quantitative appraisal of hexon gene copy number. For detection of the Ad hexon gene, the following primers and TaqMan probe were used: Ad5Hexon-fwd: 5′-TAC GCA CGA CGT GAC CAC A-3′, Ad5Hexon-rev: 5′-ATC CTC ACG GTC CAC AGG G-3′ and Ad5Hexon-probe: 5′-*6FAM*-ACC GGT CCC AGC GTT TGA CGC-*BHQ1*-3′; for human β-Actin gene expression: β-Actin-fwd: 5′-GAG GCA TCC TCA CCC TGA AG-3′, β-Actin-rev: 5′-TCC ATG TCG TCC CAG TTG GT-3′, and β-Actin-probe: 5′-*HEX*-CCC CAT CGA GCA CGG CAT CG-*BHQ1*-3′. In each reaction, 20 ng of total DNA was used as template and PCR was performed in 10 μl of reaction mixture containing 5 μl of 2x Fast Start Taq Man Probe Master Mix (Roche Applied Science, Indianapolis, IN), 333 nM each primer, and 100 nM fluorogenic probe. Amplifications were carried out in a 96-well reaction plate (PE Applied Biosystems, Grand Island, NY) in a spectrofluorimetric thermal cycler (The LightCycler® 480 Real-Time PCR System, Roche Applied Science). After the initial denaturation (2 min at 95°C), amplification was performed with 45 cycles of 15 sec at 95°C and 60 sec at 60°C. Each sample was run in triplicate. A threshold cycle (*C*t) for each triplicate was estimated by determining the point at which the fluorescence exceeded a threshold limit (10-fold the standard deviation of the baseline). Level of the CRAd binding in tested cells was determined as the Ad hexon gene copy number per 1 ng total DNA.

## CRAd replication in pancreatic tumor xenografts

AsPC-1 and AsPC-1G tumor xenografts were generated by *s.c.* transplantation to the flanks of female nude mice as described above. Tumor xenografts were injected with $1 \times 10^{10}$ vp of CRAdcxcr4H5-F5 or CRAdcxcr4H5-F5/F3. At different times after injection, the animals were humanely sacrificed by CO2 inhalation, tumor tissue was harvested, template DNA was prepared from whole tissue extracts using QIAamp DNA Mini Kit (Qiagen) and subjected to TaqMan quantitative PCR as described above. CRAd replication in human tumor xenografts was determined as the Ad hexon gene copy number per 1 ng total DNA.

### Biodistribution studies

For biodistribution experiments, athymic nude mice were injected intravenously (*i.v.*) *via* the tail vein with $1 \times 10^{10}$ vp of CRAdcxcr4H5-F5, CRAdcxcr4H5-F3, CRAdcxcr4H5-F5/F3 and CRAdcxcr4H5/3-F5/F3 recombinant Ad vectors. Five days after injection major organs were harvested and subjected to TaqMan quantitative PCR as described above.

To evaluate CRAd replication in tumor tissues, human pancreatic tumor xenografts were generated by *s.c.* injection of $14 \times 10^6$ AsPC-1 and AsPC-1G cells mixed 2:1 (v/v) with Matrigel (Collaborative Biomedical Products) to left and right flanks, respectively, of athymic nude mice as described above. Ten days after tumor cell transplantation, mice were injected *i.v.* with $1 \times 10^{10}$ vp per animal of CRAdcxcr4H5-F5, CRAdcxcr4H5-F3, CRAdcxcr4H5-F5/F3 or CRAdcxcr4H5/3-F5/F3. Five days after injection animals were humanely sacrificed by CO2 inhalation, tumors were harvested and subjected to TaqMan quantitative PCR as described above.

### Experimental therapy studies

To evaluate efficacy of combination of oncolytic virotherapy with chemotherapy, $4.5 \times 10^6$ AsPC-1G cells mixed 2:1 (v/v) with Matrigel (Collaborative Biomedical Products) were injected *s.c.* into athymic nude mice. Treatment was started 12 days post-tumor cell injection at the time of established tumor growth (tumors were 6–8 mm in diameter), noted as Day 0. Animals were randomly divided into groups receiving different treatments: 1) PBS alone; 2) gemcitabine alone; 3) CRAdcxcr4H5/3-F5/F3 and PBS; 4) CRAdcxcr4H5/3-F5/F3 and gemcitabine. Two groups (# 2 and 4) of mice received *i.p.* gemcitabine (100 mg/kg) or PBS (# 1 and 3) on Days 0, 3, 5 and 7. In groups # 3 and 4 mice were injected *i.v.* with $1 \times 10^{10}$ vp per animal CRAdcxcr4H5/3-F5/F3 on Days 2 and 9. Tumor size was monitored twice a week using calipers and tumor volumes ($0.5 \times \text{length} \times \text{width}^2$ in $\text{mm}^3$) were calculated. Mean time to tumor doubling of the group receiving different treatments was calculated.

### Statistical analysis

All error terms are expressed as the standard deviation of the mean. Significance levels for comparison of differences between groups in the *in vitro* experiments were analyzed by Student's *t* test with exact computations for *p*-value. All reported *p*-values are two-sided. In experiments where triplicates were run to reduce measurement error, the statistical analyses were conducted on the mean triplicate value. The differences between groups were considered to be statistically significant when *p*-value was less than or equal to 0.05. In the animal model tumor therapy studies, the treatment groups were compared with respect to tumor size and percent of original tumor size over time. To test for significant differences in mean time to tumor doubling between treatment groups, one-way analysis of variance (ANOVA) test was conducted. When the ANOVA indicated that a significant difference existed ($p$-value $< 0.05$), multiple comparison procedures were used to determine where the differences lay.

## RESULTS

### CXCR4 promoter activity in pancreatic cancer cell lines

A simplified schematic of recombinant Ad vector genomes used in this study is summarized in Figure 1a. To evaluate the ability of the CXCR4 promoter to drive cell-specific gene expression, human pancreatic cancer cells were infected with replication-deficient recombinant adenoviruses, Adcxcr4Luc or AdcmvLuc, encoding the firefly luciferase (Luc) gene under control of the CXCR4 or CMV promoter, respectively. Forty-eight hours after infection, cells were harvested and Luc expression was analyzed using a luciferase assay system. Variable levels of Luc expression were detected in the tested cell lines; the level of expression was increasing in proportion to the MOI (results not shown). As shown in Figure 1b, MiaPaCa-2, L3.6, Capan-1 and AsPC-1 cells demonstrated relatively high levels of Luc expression following Adcxcr4Luc infection in comparison with other tested cells, whereas HS7665 and HPAF-II cells showed the lowest levels of Luc expression following Adcxcr4Luc and AdcmvLuc infection.

### Development and evaluation of chemotherapy resistant model of pancreatic cancer

To establish chemotherapy resistant pancreatic cancer cells, Capan-1, L3.6 and AsPC-1 cells were incubated with different doses of gemcitabine. Under selective conditions, gemcitabine resistant cells outgrow non-resistant cells, resulting in a polyclonal population of chemotherapy resistant Capan-1G, L3.6G and AsPC-1G cells. These heterogeneous populations of resistant cell clones were used for experimental analysis. To determine the sensitivity of pancreatic cancer cell lines to gemcitabine, cells were treated with increasing concentrations of gemcitabine, and the cytotoxicity of this drug was determined by measuring surviving cells using the crystal violet staining method. As shown in Figure 2a, the susceptibility to cytotoxic effects of gemcitabine was variable in different pancreatic cancer cell lines. The concentration of gemcitabine to produce 50% viable cells (IC50, 50% inhibitory concentration) was 35.4 ± 8.0 nM for Capan-1 cells, 143.7 ± 29.7 nM for Capan-1G cells, 11.2 ± 3.2 nM for L3.6 cells, 328.5 ± 73.2 nM for L3.6G cells, 25.4 ± 11.3 nM for AsPC-1 cells, and 572.3 ± 97.8 nM for AsPC-1G cells.

### Gemcitabine sensitivity of human pancreatic xenografts

Taking into consideration the results of *in vitro* experiments, AsPC-1 cells, originally derived from a metastatic ascites of a patient with pancreatic adenocarcinoma, and AsPC-1G which showed a high level of chemotherapy drug resistance, were selected for subsequent animal studies of the gemcitabine sensitivity of human pancreatic tumor xenografts. The AsPC-1 or AsPC-1G cells were *s.c.* injected into the flank of athymic nude mice and tumor xenografts were allowed to grow for 10 days. Before treatment, the mean tumor sizes in groups of 10 mice at baseline were not significantly different between treatment groups ($p>0.05$), and within the treatment groups variances were not significantly different ($p>0.05$). The baseline mean and standard deviation for tumor sizes at 10 days post tumor cell injection was 120.5 ± 38.4 $mm^3$. *In vivo* tumor therapy was initiated on Day 0, which corresponded to 10 days post-tumor cell injection. Gemcitabine was administered *i.p.* at 50 mg per kg of body weight on Days 0, 3, 5 and 7. An inhibition of AsPC-1 tumor growth was noted in mice treated with gemcitabine *versus* the PBS-injected group (Figure 2b). There

were no significant differences in AsPC-1G tumor growth between groups that received gemcitabine *versus* PBS ($p>0.05$). The mean time to tumor doubling for AsPC-1-bearing mice treated with PBS, and AsPC-1G-bearing mice treated with PBS or gemcitabine were 29, 30 and 31 days, respectively; for AsPC-1-bearing animals that received gemcitabine tumors had not doubled by day 35, the last day of this study.

## Evaluation of CRAd vectors: fiber expression

We developed a panel of Ad5-based CRAd vectors expressing *E1a* gene under transcriptional control of the CXCR4 promoter element, including CRAdcxcr4H5-F5 with wild-type Ad5 fiber, fiber-chimeric CRAdcxcr4H5-F3 vector with Ad3 fiber, fiber-mosaic CRAdcxcr4H5-F5/F3 vector expressing both Ad5 and Ad3 fibers, and fiber-mosaic hexon-modified CRAdcxcr4H5/3-F5/F3 vector. A simplified schematic of recombinant CRAd genomes used in this study is summarized in Figure 3a. First, PCR analysis was used to demonstrate the incorporation of the mosaic Ad5 and Ad3 fiber gene region in CRAdcxcr4H5-F5/F3 genome. The PCR was performed using Ad5-specific primers, which anneal at 100 bp upstream and downstream of the fiber gene, and purified CRAdcxcr4H5-F5/F3 with mosaic Ad5 and Ad3 fiber genes, CRAdcxcr4H5-F3 comprising chimeric Ad3 fiber, and wild-type CRAdcxcr4H5-F5 as template. As shown in Figure 3b, the PCR analysis demonstrated the amplification of the corresponding fiber region in each of the CRAd vectors.

To evaluate the expression of the fiber proteins in the viral capsid, $5 \times 10^9$ vp of boiled and unboiled purified CRAds were loaded in each lane and subjected to SDS-PAGE followed by Western blot analysis using anti-fiber mAb. As shown in Figure 3c, genetic incorporation of mosaic fiber genes into CRAdcxcr4H5-F5/F3 produced expression of both Ad5 and Ad3 fiber molecules, with predicted molecular weights of about 62 kDa and 37 kDa, respectively, with maintained trimerization potential of fiber proteins under native conditions.

To investigate whether infection with mosaic fiber CRAdcxcr4H5-F5/F3 vector produces stable expression of both Ad5 and Ad3 fiber proteins, HEK293 cells were infected with $1 \times 10^3$ vp per cell CRAdcxcr4H5-F5/F3. Cells and culture medium were harvested at 48 hours after infection, subjected to three freeze-thaw cycles, and after centrifugation supernatants were analyzed for fiber protein expression by Western blot and mixed 1:100 (v/v) with fresh medium and used for subsequent serial infections of HEK293 cells. The results of Western blot analysis of level of fiber protein expression during of 10 cycles of reinfection with CRAdcxcr4H5-F5/F3 are summarized in Figure 3d. The results of these studies demonstrate that cell reinfection using CRAdcxcr4H5-F5/F3 with the genetically incorporated mosaic fiber produced stable expression of both Ad5 and Ad3 fiber proteins.

## Evaluation of structural integrity of CRAd virions

Next, we tested how modifications in hexon and fiber proteins of viral capsid affect the structural integrity of the CRAd virion by comparing the thermostability of CRAdcxcr4H5-F3, CRAdcxcr4H5-F5/F3 and CRAdcxcr4H5/3-F5/F3 hexon and fiber modified vectors to wild-type CRAdcxcr4H5-F5. Based on results of a preliminary study that demonstrated a

temperature-dependent decrease of Ad-mediated gene transfer [16], the viruses were preincubated at 45°C for different times before the infection of Capan-1 cells, and relative oncolytic efficiency was obtained by comparing with the cytotoxicity of unheated CRAds. As shown in Figure 4a, level of cytotoxicity of CRAdcxcr4H5-F3, CRAdcxcr4H5-F5/F3, CRAdcxcr4H5/3-F5/F3 or CRAdcxcr4H5-F5 was retained about 50% even after a 40-min incubation at 45°C. There were no significant differences in cell killing between all tested CRAds. This data indicated that modification of the fiber and hexon proteins in the viral capsid does not alter the structural stability of the recombinant viral particles.

## Expansion of CRAd tropism via initial attachment

The parental tropism of most human Ads to the primary binding coxsackie-and-adenovirus receptor (CAR) renders some cells/tissues resistant to infection via Ad serotype 5 (Ad5)-based vectors. Alternatively, a subset of adenoviruses from species B and D use non-CAR receptors for cell binding, including Ad serotype 3 (Ad3) which utilized CD46 [17], CD80/CD86 [18], desmoglein-2 (DSG-2) [19, 20] as receptors for initial attachment to the cell surface.

Based on these findings, CHO-C2 cells expressing CD46, CHO-CAR cells expressing CAR, and CHO (CD46- CAR-) cells were infected with CRAdcxcr4H5-F5, CRAdcxcr4H5-F3 or CRAdcxcr4H5-F5/F3 for one hour and Ad transduction was evaluated using quantitative PCR. As illustrated in Figure 4b, relative levels of CRAd transduction correlated with levels of CD46 or CAR expression. The copy number of hexon transcripts following infection with CRAdcxcr4H5-F5 was increased by 1.2-fold in CHO-C2 cells and 25-fold ($p$-value < 0.05) in CHO-CAR cells in comparison with CHO cells; the copy number of CRAdcxcr4H5-F3 hexon expressing Ad3 fiber alone was slightly increased in CHO-CAR and by 10-fold ($p$-value < 0.05) in CHO-C2 cells compared to CHO cells. In contrast, the CRAdcxcr4H5-F5/F3 hexon gene copy number was significantly increased in both in CHO-C2 and CHO-CAR cells by 9-fold and 20-fold ($p$-value < 0.05), respectively, in comparison with CHO cells (Figure 4b).

## Inhibition of CRAd mediated cytotoxicity by Ad5 and Ad3 knob

Additionally, to confirm a specificity of CRAd infection we evaluated Ad5 and Ad3 knob inhibition of CRAd-mediated cytotoxicity. Since previous studies demonstrated the ability of recombinant Ad knob to block binding of the corresponding adenoviral vectors or recombinant fiber protein to its receptor [15], we expressed both Ad5 and Ad3 knob and evaluated the purified proteins by Western blotting with anti-His mAb (data not shown). For this study AsPC-1G cells were pretreated with different concentrations of recombinant Ad5 and Ad3 knob or BSA at one hour prior to infection with CRAdcxcr4H5-F5, CRAdcxcr4H5-F3 or CRAdcxcr4H5-F5/F3. As shown in Figure 4c, pre-incubation with Ad5 and Ad3 knob inhibited cell killing of the corresponding CRAdcxcr4H5-F5 and CRAdcxcr4H5-F3 vectors, respectively. As expected, there was no blocking effect of incubation of AsPC-1G cells with recombinant Ad5 knob for CRAdcxcr4H5-F3-mediated cytotoxicity as well as Ad3 knob pretreatment for CRAdcxcr4H5-F5 cell killing in the same experiment. In contrast, CRAdcxcr4H5-F5/F3 infection was efficiently inhibited by recombinant Ad5 or Ad3 knob protein in a dose-dependent manner (data not shown). As shown in Figure 4c, incubation AsPC-1G cells with 100 mg/ml of Ad5 or Ad3 knob resulted

in ~79% and 68% decreased cell killing, respectively, in comparison with BSA-treated cells following infection with mosaic CRAdcxcr4H5-F5/F3 vector expressing both Ad5 and Ad3 fibers.

### Validation of CRAd replication in human pancreatic tumor xenografts

To evaluate whether utilization of the fiber mosaicism targeting approach can alter CRAd propagation *in vivo*, AsPC-1 and AsPC-1G human pancreatic tumor xenografts were injected *i.t.* with $1 \times 10^{10}$ vp of CRAdcxcr4H5-F5 or CRAdcxcr4H5-F5/F3. Tumor tissues were collected on days 1 and 5 after injection and viral titer was measured by quantitative PCR. As seen in Figure 5a**,** there was a time-dependent increase of the copy number of hexon transcripts following injection with CRAdcxcr4H5-F5 or CRAdcxcr4H5-F5/F3 in both AsPC-1 and AsPC-1G tumors. There were significantly greater hexon gene copy numbers for CRAdcxcr4H5-F5/F3 at day 5 after injection in both AsPC-1 and AsPC-1G tumors by 29-fold and 32-fold, respectively ($p$-value < 0.05), in comparison with levels of hexon gene expression on day 1. In contrast, levels of hexon gene expression at day 1 after CRAdcxcr4H5-F5 injection were increased by 2-fold and 5-fold in AsPC-1 and AsPC-1G tumors, respectively ($p$-values > 0.05). In comparison with levels of hexon gene expression following CRAdcxcr4H5-F5/F3 injection, there was a 3-fold and 6-fold ($p$-value < 0.05) increase in the copy number of hexon transcripts at 5 days following injection with CRAdcxcr4H5-F5 in comparison with levels of hexon gene expression on day 1.

### Quantitative analysis of CRAd hexon gene expression in vivo

Recently it was shown that liver transduction of Ad5 is mediated by a high-affinity interaction between the major protein in the Ad5 capsid, hexon, and γ-carboxylated glutamic acid (Gla) domain of coagulation factor X (FX). The Ad5-FX complex attaches to hepatocytes through the binding of the serine protease domain of FX to cell surface heparan sulfate proteoglycans (HSPGs) [21–23]. Early studies demonstrated that ablation of FX binding to Ads with modified hexon protein resulted in decreased liver tropism [24–26].

To investigate whether modifications in CRAd hexon can decrease the liver sequestration and as a consequence alter CRAd biodistribution, liver and spleen were harvested after systemic administration of CRAd vectors. To confirm distribution of viral particles *in vivo*, the number of Ad hexon gene copies was measured by quantitative PCR in organs at 5 days following *i.v.* injection with CRAdcxcr4H5-F3, CRAdcxcr4H5-F5/F3, CRAdcxcr4H5/3-F5/F3 or CRAdcxcr4H5-F5. As illustrated in Figure 5b, differing levels of hexon gene expression were detected in organs after systemic administration of the various CRAd vectors. Adenoviral hexon gene copy numbers in the liver were significantly lower after injection with CRAdcxcr4H5-F3, CRAdcxcr4H5-F5/F3 and CRAdcxcr4H5/3-F5/F3 by 6-, 5- and 9-fold, respectively, compared to CRAdcxcr4H5-F5. In contrast, hexon gene expression in the spleen was significantly higher following *i.v.* injection with CRAdcxcr4H5-F3, CRAdcxcr4H5-F5/F3 and CRAdcxcr4H5/3-F5/F3 by 10-, 9- and 74-fold, respectively, compared to CRAdcxcr4H5-F5 (Figure 5c). Thus, to quantify effects of CRAd hexon modifications on biodistribution of CRAd viral particles we used the spleen-to-liver ratio of hexon gene expression. Spleen-to-liver ratios were calculated for each individual animal with the hexon gene copy number normalized by the DNA concentration

of the tissue lysates. The decrease of the liver sequestration and enhanced hexon gene expression in the spleen resulted in increased spleen-to-liver ratios of Ad hexon gene copy numbers following *i.v.* injection with CRAdcxcr4H5-F3, CRAdcxcr4H5-F5/F3 and CRAdcxcr4H5/3-F5/F3 by 56-, 48- and 600-fold, respectively, compared to CRAdcxcr4H5-F5.

## Validation of CRAd replication in human pancreatic tumor xenografts following systemic administration

For evaluation of CRAd replication *in vivo*, mice bearing *s.c.* AsPC-1 and AsPC-1G human pancreatic tumor xenografts were injected *via* tail vein with CRAdcxcr4H5-F3, CRAdcxcr4H5-F5/F3, CRAdcxcr4H5/3-F5/F3 or CRAdcxcr4H5-F5 vectors. At 5 days after injection, tumors were harvested and number of Ad hexon gene copies in tumor tissues were measured by quantitative PCR. Additionally, we calculated ratios of hexon gene copy number in tumor tissue lysates for AsPC-1G to AsPC-1 xenografts in each individual animal. Average ratios for all the individual sets of numbers for different groups of mice were compared. As shown in Figure 5d, CRAd replication was detected in both AsPC-1 and AsPC-1G human pancreatic tumor xenografts, and modifications of viral capsid resulted in increased CRAd replication in AsPC-1G tumor xenografts and improved AsPC-1G to AsPC-1 ratio by 8-, 7- and 6-fold following *i.v.* injection with CRAdcxcr4H5-F3, CRAdcxcr4H5-F5/F3 and CRAdcxcr4H5/3-F5/F3, respectively, compared to CRAdcxcr4H5-F5 (Figure 5e).

## Efficacy of combination of oncolytic virotherapy with chemotherapy in a human pancreatic tumor xenograft model

Taking into consideration the results of previous experiments, AsPC-1G cells were selected for subsequent animal studies of combined oncolytic virotherapy with chemotherapy as they were the most resistant to *in vitro* treatment with gemcitabine and thus provided the most stringent test of the efficacy of this therapy. Also, based on data not shown from an *in vivo* gemcitabine dose-escalation study, the maximum tolerated dose of gemcitabine at 100 mg/kg, administered *i.p.* four times for one week, was chosen to evaluate the therapeutic potential of combination oncolytic virotherapy with chemotherapy *in vivo*. AsPC-1G cells were *s.c.* injected into the flank of athymic nude mice. Before treatment, the mean tumor sizes in groups of 10 mice at baseline were not significantly different between treatment groups ($p>0.05$), and the within treatment variances were not significantly different ($p>0.05$). The baseline mean and standard deviation for tumor sizes at 12 days post tumor cell injection was $178.1 \pm 53.7$ $mm^3$. *In vivo* tumor therapy was initiated on Day 0, which corresponded to 12 days post-tumor cell injection. Gemcitabine was administered *i.p.* at 100 mg/kg on Days 0, 3, 5 and 7. Animals were injected *i.v.* with $1 \times 10^{10}$ vp CRAdcxcr4H5/3-F5/F3 on Days 2 and 9. An inhibition of AsPC-1G tumor growth was noted in groups of mice treated with CRAdcxcr4H5/3-F5/F3 plus PBS and CRAdcxcr4H5/3-F5/F3 in combination with gemcitabine treatment *versus* gemcitabine alone (Figure 5f). The mean time to tumor doubling for PBS alone, gemcitabine alone, CRAdcxcr4H5/3-F5/F3 plus PBS and CRAdcxcr4H5/3-F5/F3 plus gemcitabine treatment groups were 15, 17, 29 and 37 days, respectively. There were no significant differences in tumor growth between groups that received gemcitabine alone *versus* PBS alone, CRAdcxcr4H5/3-F5/F3 plus PBS, *versus*

CRAdcxcr4H5/3-F5/F3 plus gemcitabine ($p>0.05$). Comparisons of mean time to tumor doubling of the group treated with CRAdcxcr4H5/3-F5/F3 plus PBS or CRAdcxcr4H5/3-F5/F3 in combination with gemcitabine *versus* gemcitabine alone showed significant differences between the groups ($p<0.05$).

## DISCUSSION

In this initial study we sought to establish the key feasibilities relevant to the successful derivation and validation of a novel oncolytic Ad agent based on fiber modification. A panel of CRAd vectors has been derived which embodies two fibers from Ad5 and Ad3 to achieve complex mosaicism for inclusion targeting, the CXCR4 promoter for conditional replication, and hexon HVR7 modification for liver untargeting. Obtained data demonstrate efficacious targeting and replication of CRAds *in vitro* and *in vivo* using a chemoresistant model of pancreatic cancer. Importantly, CRAd vector modified in this manner, and delivered using the systemic route, improved anti-tumor efficacy of experimental oncolytic therapy in combination with gemcitabine of chemoresistant pancreatic xenografts.

Pancreatic cancer is the fourth leading cause of cancer death, and the eighth most frequent type of solid tumor in North America [1]. Despite significant efforts little progress has been made in the treatment of this disease. It is clear that new approaches are needed for pancreatic cancer therapy. A major effort is ongoing for the development of new therapeutics, including molecular targeted drugs, natural compounds, therapeutic antibodies, gene therapies, and virotherapy [27, 28]. A very promising targeted therapy for the treatment of neoplastic diseases is the utilization of viral agents. In this regard, multiple gene therapy and virotherapy interventions have been rapidly applied to the context of pancreatic cancer in response to the desperate need for an effective therapy for this devastating disease (reviewed in [27]). However, design advancements in current virotherapy agents are required to optimize their therapeutic index and to address chemoresistant disease.

Our point-of-departure for the design of an optimized CRAd agent for pancreatic cancer embodied the following concepts for the successful development of a pancreatic tumor-targeted CRAd: 1) specific and effective transduction of pancreatic cancer cells; 2) selective replication in tumor and tumor-associated cells; and 3) optimal biodistribution following systemic administration. Most importantly, we sought a strategy based on the design of a CRAd which could infect a heterogeneous tumor cell population. Thus, vector particles must therefore embody the potential for targeting distinct cellular targets. In this early proof-of-concept study, we sought to employ the “complex mosaic” approach and develop CRAd vectors that inclusively target the general and heterogeneous tumor cell population. We hypothesized that “inclusively targeting” of the heterogeneous tumor cell population will result in an increased anti-tumor efficacy of CRAd mediated oncolytic virotherapy. To achieve this, we developed a strategy of capsid modification whereby single particles can incorporate multiple and distinct fiber species. Of note, in a mixed cell population displaying both Ad5 or Ad3 receptors, the mosaic Ad was capable of infecting both populations [29]. As proof-of-principle, we derived such a complex mosaic CRAd vector which embodied fibers from both serotypes Ad5 and Ad3. After rescue and propagation CRAds were subjected to studies of structural stability using thermostability analysis. These studies confirmed that the

hexon and fiber modifications did not adversely affect viral particle stability. Importantly, *in vitro* studies in serial passage validated the stability of two fiber phenotype – relative proportions of fiber Ad5 and Ad3 remained co-equal after passaging. Genetic incorporation of two fibers with different receptors for cell binding, CAR for Ad5 fiber, and CD46 [17], CD80/CD86 [18], DSG-2 [19, 20] for Ad3 fiber, allows expanded tropism of CRAd infection and provides the technical means to accomplish the goal of "inclusion targeting" required of a strategy to target a heterogeneous population of pancreatic tumor cells. Recently, it was shown that dodecahedral particles, formed by excess amounts of Ad3 capsid proteins, fiber and penton base during viral replication, can trigger DSG-2–mediated opening of intercellular junctions and increase access to a variety of cell surface receptors involved in viral spread, e.g. CD46 [20]. Results of our study demonstrate that CRAdcxcr4H5-F5/F3 and CRAdcxcr4H5/3-F5/F3 displaying both Ad5 and Ad3 fibers can utilize a number of cell surface targets as putative attachment receptors that facilitate further reinfection and lateral spreading of mosaic CRAds.

To initially validate the compatibility of this approach with complex tropism modifications, we derived an infectivity-enhanced CRAd with replicative specificity achieved using replacement of the adenoviral E1A promoter with the CXCR4 promoter element. The CXCR4 overexpression correlates with tumor growth and metastatic activity in pancreatic cancer [30]. It was shown that there was deregulation of CXCR4 expression in both pancreatic cancer and pancreatic tumor-associated cells [30, 31] suggesting this targeting axis for a dual targeted CRAd. Emerging evidence has shown that pancreatic CSCs are endowed with the ability for long-term maintenance of tumor growth as well as the formation of tumor metastases [32]. CSCs are generally the lowest replicating cancer cell population in the tumor [33].

However, conventional therapeutic regimens have not been able to effectively target and treat this stem cell population because of their intrinsically resistant nature [4, 31]. Importantly, the expression of CXCR4 is a signature of pancreatic CSCs and is up-regulated in advanced, invasive pancreatic cancer and metastases [31]. In the initial study using a panel of human pancreatic cancer cells, the CXCR4 promoter achieved high levels of reporter gene expression in undifferentiated pancreatic carcinoma MiaPaCa-2 cells, Capan-1 cells, derived from liver metastatic tissues of a patient with pancreatic adenocarcinoma, as well as in L3.6 and AsPC-1 cells which are reported to be valid models of pancreatic CSCs [31].

Additionally, we wished to address the issue of hepatic sequestration of CRAd vectors which would confound systemic delivery schemes. In this regard, it has been recently shown that interaction of serum factor X (FX) constituted the biologic basis of this phenomenon [22, 24]. Although not universally accepted, the major pathway of liver transduction involves interactions between the Ad5 hexon-FX complex and cell surface of hepatocytes. Early studies determined that ablation of FX binding to Ads with modified hexon from Ad serotypes with relatively low affinity to FX in comparison with Ad5 resulted in decreased liver tropism [24–26]. We thus derived a CRAd vector chimeric for a hexon with substitution of the HVR7 of the Ad5 hexon with HVR7 from Ad serotype 3. Of note, this alteration mitigated hepatic sequestration of systemically administered Ad and dramatically altered biodistribution of gene expression [16]. In this study it could be seen that the capsid

modification dramatically enhanced the spleen-to-liver ratio of copy number Ad hexon transcripts by ~50-fold following injection with CRAdcxcr4H5-F3 comprising chimeric Ad3 fiber, and CRAdcxcr4H5-F5/F3 displaying mosaic Ad5 and Ad3 fibers, as well as 600-fold following injection with mosaic CRAdcxcr4H5/3-F5/F3 expressing chimeric hexon in comparison with wild-type CRAdcxcr4H5-F5. Recent studies have revealed that association of Ad5 hexon with FX resulted in innate immunity activation [34] as well as that Ad5-FX interaction protected from antibody- and complement-mediated neutralization in murine experimental models [35]. The complexity of interaction of Ad5-based CRAds with the host resulted in only a modest increase in the absolute levels of viral replication in the tumor xenografts in comparison with a profound increase in the spleen-to-liver ratio of Ad hexon gene expression in the liver following systemic administration of hexon-modified CRAd vectors.

Also, modifications of viral capsid resulted in increased viral replication in AsPC-1G tumor xenografts and improved AsPC-1G to AsPC-1 ratio in comparison with wild-type CRAdcxcr4H5-F5 vector. Our studies showed that the complex mosaic CRAd could infect pancreatic cancer cells using the receptor for Ad5 and Ad3. However, additional experiments, that are beyond the scope of this study, are required to investigate molecular mechanisms of mosaic CRAd-mediated oncolysis. For validation of the stability of the two-fiber phenotype of the complex mosaic CRAd in the context of multiple cycles of viral replication in the *in vivo* model of subcutaneous human tumor xenograft provides appropriate biologic substrate. To address anti-tumor efficacy gains, however, this model system would not be useful. Specifically, improved efficacy based on inclusion targeting requires fiber binding efficacy for tumor and stromal elements. The widely employed subcutaneous human tumor xenograft model embodies murine stroma elements in conjunction with human tumor cells. The limited binding efficacy of the fiber knob of human Ad serotype 3 for murine tissue would undermine any analysis based upon two-fiber functionality [20, 36].

The combination of CRAd virotherapy with chemotherapy should provide a major advantage to achieve a higher therapeutic result by using low doses of oncolytic virus and chemotherapy. Finally, we investigated whether a combination of oncolytic virotherapy and chemotherapy using gemcitabine produces increased cytotoxicity against chemoresistant tumor cells in comparison with these agents alone. Combination of CRAdcxcr4H5/3-F5/F3 and gemcitabine significantly inhibited AsPC-1G tumor growth in comparison with gemcitabine alone. Thus, the combination of both tropism modification of CRAd with CXCR4 controlled replication can achieve an anti-tumor effect. In this study the maximum tolerated dose of gemcitabine was used to investigate the therapeutic effect of this drug alone *versus* in combination with oncolytic virotherapy. However, the mean time to tumor doubling for CRAdcxcr4H5/3-F5/F3 plus gemcitabine was increased by 8 days versus CRAdcxcr4H5/3-F5/F3 alone, in comparison with only 2 days for gemcitabine alone versus PBS alone, probably, due to the high level of chemotherapy resistance of AsPC-1G tumor cells. To our knowledge, this is the first demonstration of a complex mosaic CRAd vector which contains fibers derived from both Ad serotype 5 and serotype 3 that is used for experimental virotherapy of chemoresistant pancreatic cancer. The experimental therapy of

pancreatic cancer has shown that CRAd vector is compatible and effective in combination with chemotherapy using gemcitabine. Although our initial data with the complex mosaic CRAd are promising, optimization of the experimental therapy regimen is also required.

In conclusion, we used an infectivity-enhanced CXCR4 promoter-based CRAd vector with the ability to produce pancreatic cancer cell killing using the receptor for Ad5 and Ad3. The application of such strategies that combine oncolytic virotherapy with chemotherapy using a CRAd vector with tropism expansion for targeting of a heterogeneous tumor cell population and hexon modifications for liver untargeting, offers unique opportunities to develop a more effective pancreatic cancer therapy. This study thus highlights the efficacy gains that may accrue to additional advancements in the design of CRAd agents along the lines we have demonstrated here.

## Acknowledgments

The authors thank Cynthia L. Marich from the Biologic Therapeutics Center, Department of Radiation Oncology, School of Medicine, Washington University in St. Louis for her assistance in preparing the manuscript. This work was supported in part by the National Institutes of Health under award number 5P50 CA101955.

## References

1. Siegel R, Ma J, Zou Z, Jemal A. Cancer statistics, 2014. CA Cancer J Clin. 2014; 64 (1):9–29. [PubMed: 24399786]
2. Neesse A, Krug S, Gress TM, Tuveson DA, Michl P. Emerging concepts in pancreatic cancer medicine: targeting the tumor stroma. Onco Targets Ther. 2013; 7:33–43. [PubMed: 24379681]
3. Lowery MA, O'Reilly EM. Genomics and pharmacogenomics of pancreatic adenocarcinoma. Pharmacogenomics J. 2012; 12(1):1–9. [PubMed: 22186617]
4. Shah AN, Summy JM, Zhang J, Park SI, Parikh NU, Gallick GE. Development and characterization of gemcitabine-resistant pancreatic tumor cells. Ann Surg Oncol. 2007; 14(12):3629–37. [PubMed: 17909916]
5. Gourgou-Bourgade S, Bascoul-Mollevi C, Desseigne F, Ychou M, Bouche O, Guimbaud R, et al. Impact of FOLFIRINOX compared with gemcitabine on quality of life in patients with metastatic pancreatic cancer: results from the PRODIGE 4/ACCORD 11 randomized trial. J Clin Oncol. 2013; 31(1):23–9. [PubMed: 23213101]
6. Von Hoff DD, Ervin T, Arena FP, Chiorean EG, Infante J, Moore M, et al. Increased survival in pancreatic cancer with nab-paclitaxel plus gemcitabine. N Engl J Med. 2013; 369(18):1691–703. [PubMed: 24131140]
7. Yamamoto M, Curiel DT. Cancer gene therapy. Technol Cancer Res Treat. 2005; 4(4):315–30. [PubMed: 16029053]
8. Eager RM, Nemunaitis J. Clinical development directions in oncolytic viral therapy. Cancer Gene Ther. 2011; 18(5):305–17. [PubMed: 21436867]
9. Tan BT, Park CY, Ailles LE, Weissman IL. The cancer stem cell hypothesis: a work in progress. Lab Invest. 2006; 86(12):1203–7. [PubMed: 17075578]
10. Dalerba P, Cho RW, Clarke MF. Cancer stem cells: models and concepts. Annu Rev Med. 2007; 58:267–84. [PubMed: 17002552]
11. Li C, Heidt DG, Dalerba P, Burant CF, Zhang L, Adsay V, et al. Identification of pancreatic cancer stem cells. Cancer Res. 2007; 67(3):1030–7. [PubMed: 17283135]
12. Abel EV, Simeone DM. Biology and clinical applications of pancreatic cancer stem cells. Gastroenterology. 2013; 144(6):1241–8. [PubMed: 23622133]
13. Zhu ZB, Makhija SK, Lu B, Wang M, Kaliberova L, Liu B, et al. Transcriptional targeting of adenoviral vector through the CXCR4 tumor-specific promoter. Gene Ther. 2004; 11(7):645–8. [PubMed: 15029227]

14. He TC, Zhou S, da Costa LT, Yu J, Kinzler KW, Vogelstein B. A simplified system for generating recombinant adenoviruses. Proc Natl Acad Sci U S A. 1998; 95 (5):2509–14. [PubMed: 9482916]
15. Krasnykh VN, Mikheeva GV, Douglas JT, Curiel DT. Generation of recombinant adenovirus vectors with modified fibers for altering viral tropism. J Virol. 1996; 70(10):6839–46. [PubMed: 8794325]
16. Kaliberov SA, Kaliberova LN, Hong Lu Z, Preuss MA, Barnes JA, Stockard CR, et al. Retargeting of gene expression using endothelium specific hexon modified adenoviral vector. Virology. 2013; 447(1–2):312–25. [PubMed: 24210128]
17. Sirena D, Lilienfeld B, Eisenhut M, Kalin S, Boucke K, Beerli RR, et al. The human membrane cofactor CD46 is a receptor for species B adenovirus serotype 3. J Virol. 2004; 78(9):4454–62. [PubMed: 15078926]
18. Short JJ, Vasu C, Holterman MJ, Curiel DT, Pereboev A. Members of adenovirus species B utilize CD80 and CD86 as cellular attachment receptors. Virus Res. 2006; 122(1–2):144–53. [PubMed: 16920215]
19. Tuve S, Wang H, Ware C, Liu Y, Gaggar A, Bernt K, et al. A new group B adenovirus receptor is expressed at high levels on human stem and tumor cells. J Virol. 2006; 80(24):12109–20. [PubMed: 17020944]
20. Wang H, Li ZY, Liu Y, Persson J, Beyer I, Moller T, et al. Desmoglein 2 is a receptor for adenovirus serotypes 3, 7, 11 and 14. Nat Med. 2011; 17(1):96–104. [PubMed: 21151137]
21. Parker AL, Waddington SN, Nicol CG, Shayakhmetov DM, Buckley SM, Denby L, et al. Multiple vitamin K-dependent coagulation zymogens promote adenovirus-mediated gene delivery to hepatocytes. Blood. 2006; 108(8):2554–61. [PubMed: 16788098]
22. Shayakhmetov DM, Gaggar A, Ni S, Li ZY, Lieber A. Adenovirus binding to blood factors results in liver cell infection and hepatotoxicity. J Virol. 2005; 79(12):7478–91. [PubMed: 15919903]
23. Zinn KR, Szalai AJ, Stargel A, Krasnykh V, Chaudhuri TR. Bioluminescence imaging reveals a significant role for complement in liver transduction following intravenous delivery of adenovirus. Gene Ther. 2004; 11(19):1482–6. [PubMed: 15295616]
24. Alba R, Bradshaw AC, Parker AL, Bhella D, Waddington SN, Nicklin SA, et al. Identification of coagulation factor (F)X binding sites on the adenovirus serotype 5 hexon: effect of mutagenesis on FX interactions and gene transfer. Blood. 2009; 114(5):965–71. [PubMed: 19429866]
25. Alba R, Bradshaw AC, Coughlan L, Denby L, McDonald RA, Waddington SN, et al. Biodistribution and retargeting of FX-binding ablated adenovirus serotype 5 vectors. Blood. 2010; 116(15):2656–64. [PubMed: 20610817]
26. Short JJ, Rivera AA, Wu H, Walter MR, Yamamoto M, Mathis JM, et al. Substitution of adenovirus serotype 3 hexon onto a serotype 5 oncolytic adenovirus reduces factor X binding, decreases liver tropism, and improves antitumor efficacy. Mol Cancer Ther. 2010; 9(9):2536–44. [PubMed: 20736345]
27. Prados J, Alvarez PJ, Melguizo C, Rodriguez-Serrano F, Carrillo E, Boulaiz H, et al. How is gene transfection able to improve current chemotherapy? The role of combined therapy in cancer treatment. Curr Med Chem. 2012; 19(12):1870–88. [PubMed: 22414080]
28. Xu C, Li H, Su C, Li Z. Viral therapy for pancreatic cancer: tackle the bad guys with poison. Cancer Lett. 2013; 333(1):1–8. [PubMed: 23354590]
29. Takayama K, Reynolds PN, Short JJ, Kawakami Y, Adachi Y, Glasgow JN, et al. A mosaic adenovirus possessing serotype Ad5 and serotype Ad3 knobs exhibits expanded tropism. Virology. 2003; 309(2):282–93. [PubMed: 12758175]
30. Wehler T, Wolfert F, Schimanski CC, Gockel I, Herr W, Biesterfeld S, et al. Strong expression of chemokine receptor CXCR4 by pancreatic cancer correlates with advanced disease. Oncol Rep. 2006; 16(6):1159–64. [PubMed: 17089032]
31. Hermann PC, Huber SL, Herrler T, Aicher A, Ellwart JW, Guba M, et al. Distinct populations of cancer stem cells determine tumor growth and metastatic activity in human pancreatic cancer. Cell Stem Cell. 2007; 1(3):313–23. [PubMed: 18371365]
32. Castellanos JA, Merchant NB, Nagathihalli NS. Emerging targets in pancreatic cancer: epithelial-mesenchymal transition and cancer stem cells. Onco Targets Ther. 2013; 6:1261–7. [PubMed: 24049451]

33. Ribacka C, Hemminki A. Virotherapy as an approach against cancer stem cells. Curr Gene Ther. 2008; 8(2):88–96. [PubMed: 18393830]

34. Doronin K, Flatt JW, Di Paolo NC, Khare R, Kalyuzhniy O, Acchione M, et al. Coagulation factor X activates innate immunity to human species C adenovirus. Science. 2012; 338(6108):795–8. [PubMed: 23019612]

35. Xu Z, Qiu Q, Tian J, Smith JS, Conenello GM, Morita T, et al. Coagulation factor X shields adenovirus type 5 from attack by natural antibodies and complement. Nat Med. 2013; 19(4):452–7. [PubMed: 23524342]

36. Wang H, Beyer I, Persson J, Song H, Li Z, Richter M, et al. A new human DSG2-transgenic mouse model for studying the tropism and pathology of human adenoviruses. J Virol. 2012; 86(11):6286–302. [PubMed: 22457526]

Figure 1A

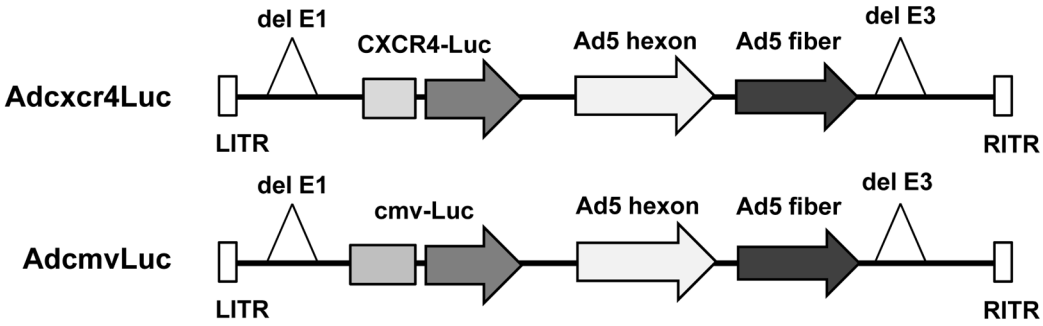


Figure 1B

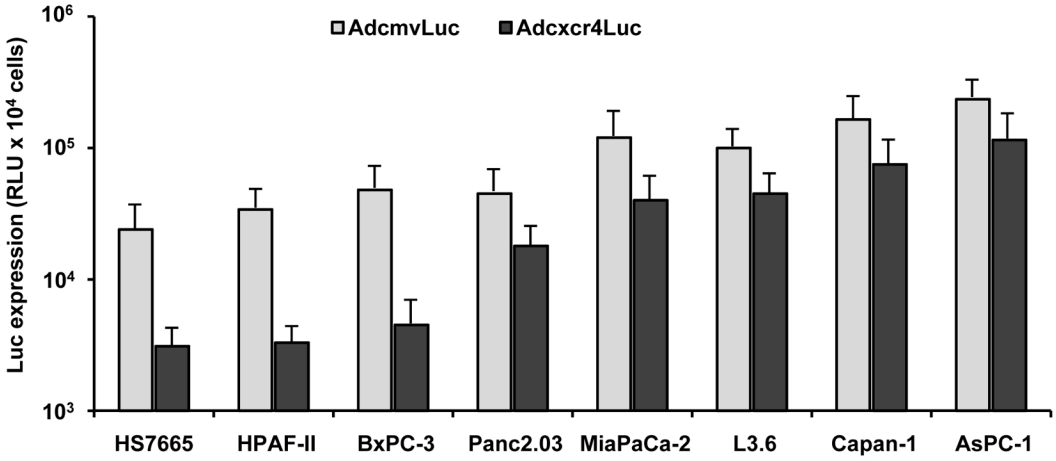


**Figure 1.**

Initial evaluation of CXCR4 promoter activity in pancreatic cancer cell lines. (**a**). Simplified schematic of recombinant Ad vector genomes used in this study. Only genomic regions relevant to presented studies are highlighted. (**b**) Relative Luc expression following infection with Adcxcr4Luc as compared to AdcmvLuc. Luciferase activity was detected in the lysates of infected cells at 48 hours after infection. Data are presented as relative light units (RLU) per $1 \times 10^4$ cells and bars represent the mean + standard deviations (s.d.) of three independent experiments, each performed in three replicates.

**Figure 2A**

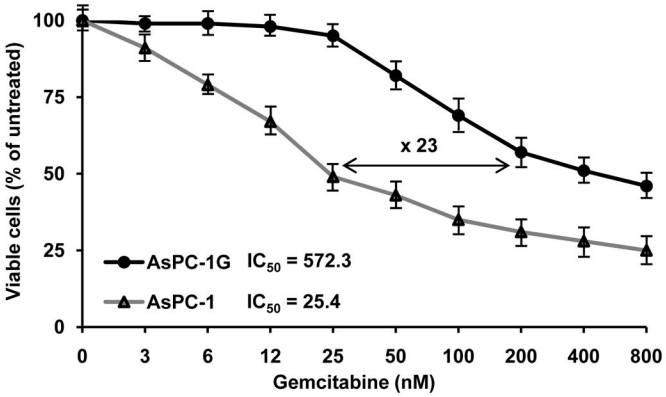


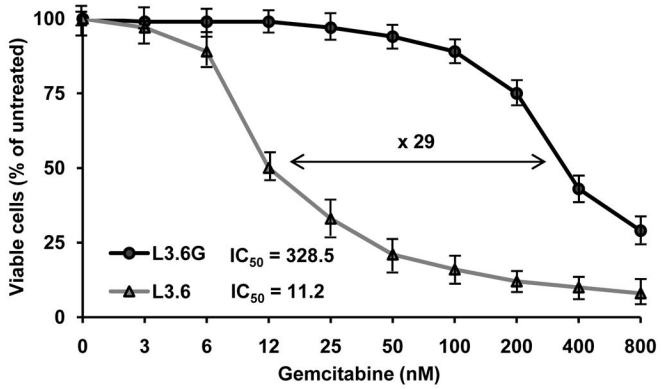


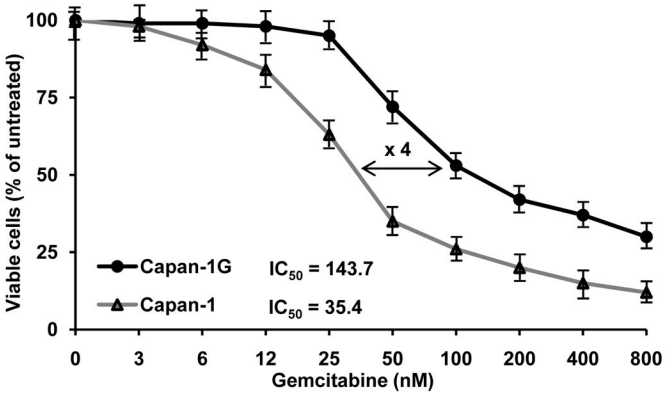

Figure 2B

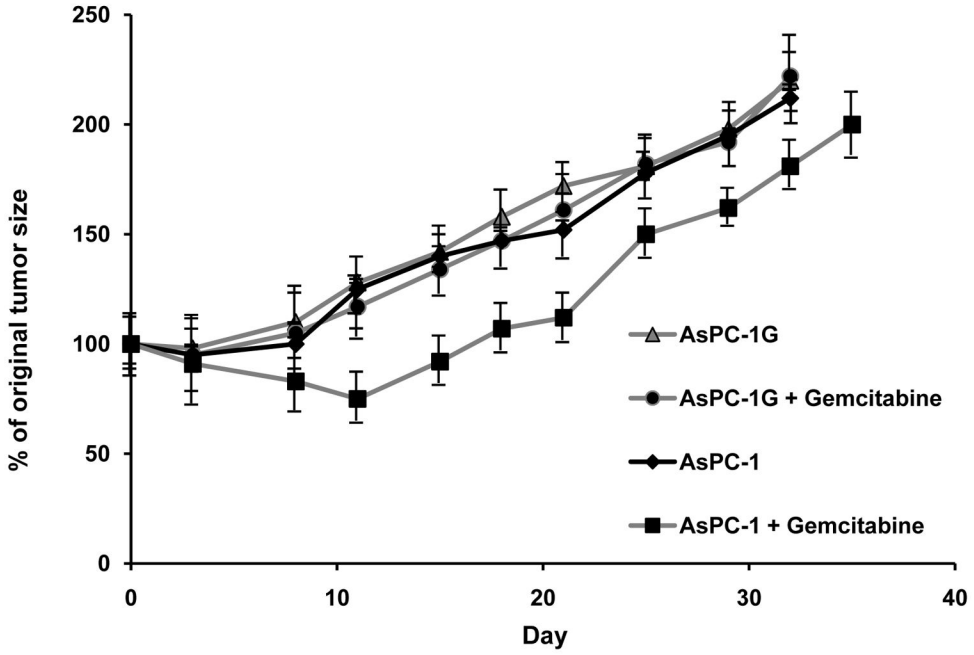


**Figure 2.**

Evaluation of chemotherapy resistant pancreatic cancer cells. (**a**). Gemcitabine cytotoxicity *in vitro*. Human pancreatic cancer cells were treated with serial dilutions of gemcitabine. Cell viability was determined using the crystal violet staining assay. Number of viable cells is given as a percentage of the number in the presence of gemcitabine compared with mock-treated cells. Presented are mean values + s.d. of three independent experiments, each performed in ten replicates. (**b**) The effect of gemcitabine treatment on tumor growth in athymic nude mice bearing *s.c.* pancreatic cancer xenografts. Gemcitabine was administered *i.p*. at 50 mg per kg of body weight on Days 0, 3, 5 and 7. An inhibition of tumor growth was noted only in mice bearing *s.c.* AsPC-1 xenografts treated with gemcitabine *versus* the PBS-injected group.

**Figure 3A**

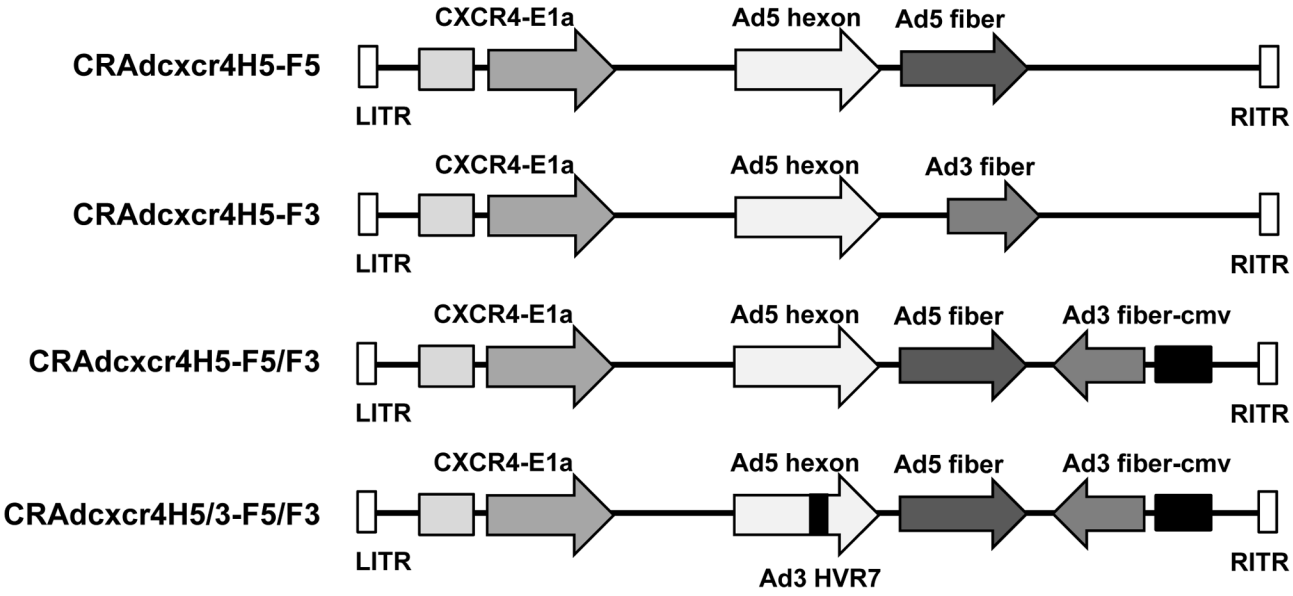

Figure 3B

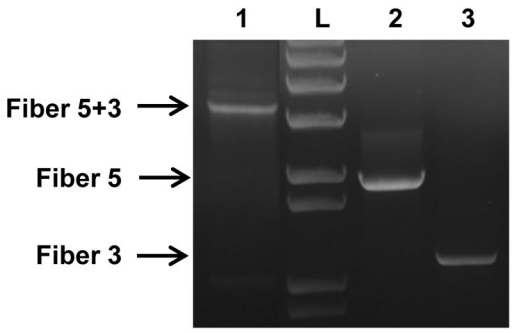


Figure 3C

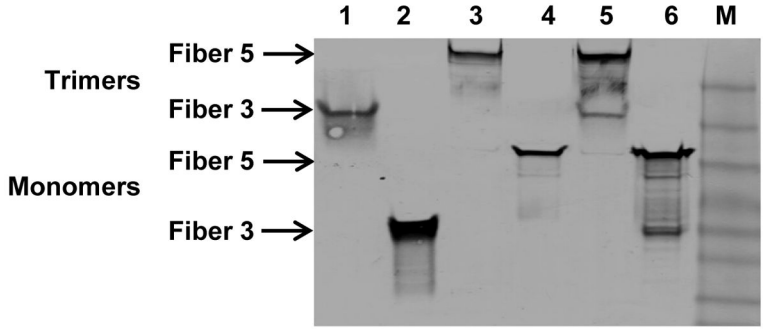


Figure 3D

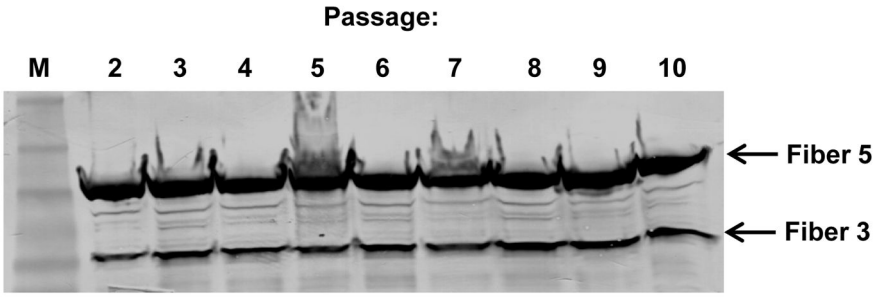


**Figure 3.**

Validation of fiber expression of CRAd vectors. (**a**). Simplified schematic of recombinant CRAd vector genomes used in this study. Only genomic regions relevant to presented studies are highlighted. (**b**). Evaluation of incorporation of fiber genes into CRAd genome. Viral genomic DNA was extracted from purified viral stock and subjected to PCR analysis. PCR products including CRAdcxcr4H5-F5/F3 (line 1) CRAdcxcr4H5-F5 (line 2) and CRAdcxcr4H5-F3 (line 3) were analyzed by 1% agarose electrophoresis with ethidium bromide staining. One representative of two different experiments is shown. (**c**) Evaluation of incorporation of fiber proteins into Ad particles using Western blotting analysis. Equal

amounts ($5 \times 10^9$ vp) of purified CRAd vectors including CRAdcxcr4H5-F3 (lanes 1 and 2), CRAdcxcr4H5-F5 (lanes 3 and 4), and CRAdcxcr4H5-F5/F3 (lanes 5 and 6) were loaded in each lane with boiling in a sample buffer (lanes 1, 3, and 5) or without boiling (lanes 2, 4 and 6) and separated on SDS-PAGE followed by transfer to a PVDF membrane. Fiber protein expression was detected using anti-fiber mAb. One representative of three different experiments is shown. (**d**) Evaluation of stability of Ad5 and Ad3 fiber protein expression. Equal volumes of lysates of HEK293 cells reinfected with CRAdcxcr4H5-F5/F3 from different passages were loaded in each lane with boiling in a sample buffer and separated on SDS-PAGE followed by transfer to a PVDF membrane and Western blotting analysis using anti-fiber mAb.

**Figure 4A**

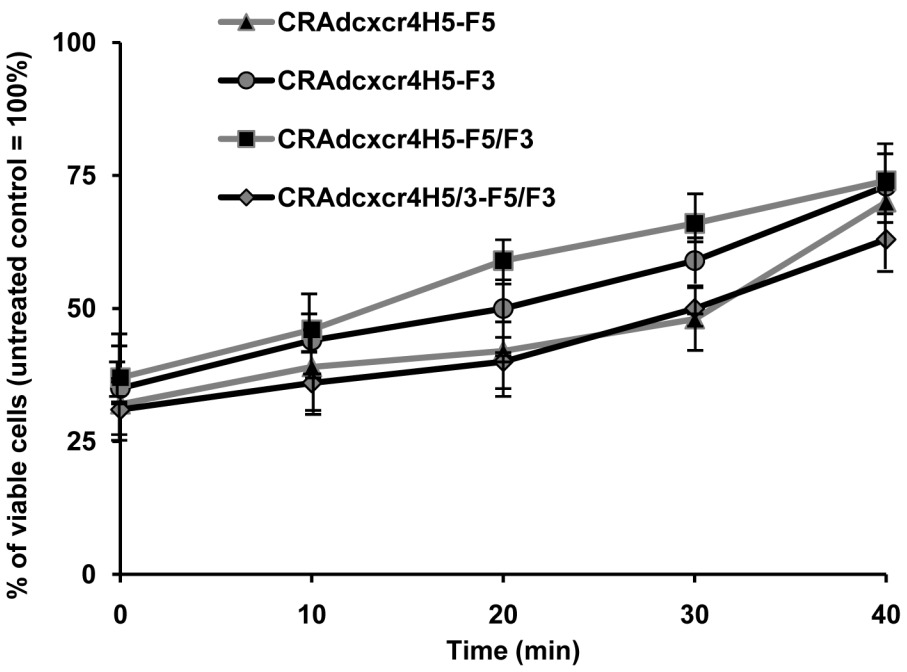

**Figure 4B**

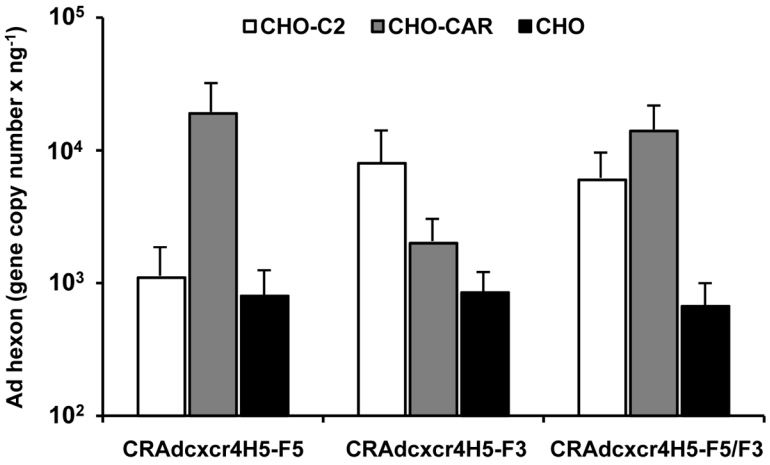


**Figure 4C**

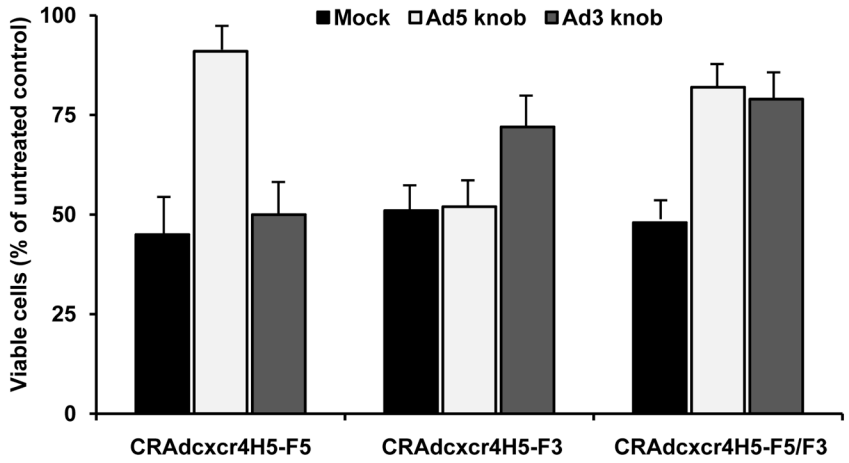


**Figure 4.**

*In vitro* characterization of CRAd vectors. (**a**) Thermostability of CRAd vectors. The viruses were incubated at 45°C for different time intervals before the infection of Capan-1 cells. Ninety-six hours after infection cells were subjected to crystal violet staining. Relative density of adherent cells was obtained by changing the OD595 readings of cells infected with the heat-treated viruses to the percentage of the readings of untreated viruses and the OD595 value of blank wells was subtracted. Presented are mean values + s.d. of three independent experiments, each performed in ten replicates. (**b**) Evaluation of expansion of CRAd tropism via initial attachment. CHO-C2 (CD46+), CHO-CAR (hCAR+), and CHO

cells were infected with CRAdcxcr4H5-F5, CRAdcxcr4H5-F3 or CRAdcxcr4H5-F5/F3 for one hour and CRAd transduction was evaluated using quantitative PCR. Presented are mean values of Ad hexon gene copy number per ng of total DNA + s.d. of two independent experiments, each performed in duplicates. (**c**) Evaluation of specificity of the CRAd infection. AsPC-1G cells were preincubated with 100 mg/ml of recombinant Ad5 or Ad3 fiber knob proteins or BSA and infected with $1 \times 10^3$ vp per cell of CRAdcxcr4H5-F5, CRAdcxcr4H5-F3 or CRAdcxcr4H5-F5/F3. Cytotoxicity of CRAd infection was determined using a crystal violet staining assay. Number of viable cells is given as percentages of the cell number in presence of Ad5 or Ad3 fiber knob compared with PBS-treated cells. Presented are mean values + s.d. of two independent experiments, each performed in ten replicates.

**Figure 5A**

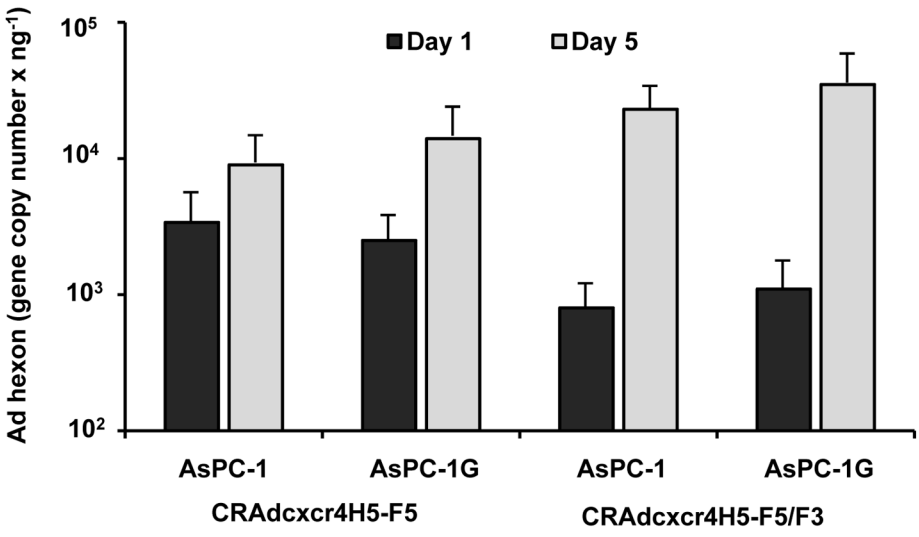

**Figure 5B**

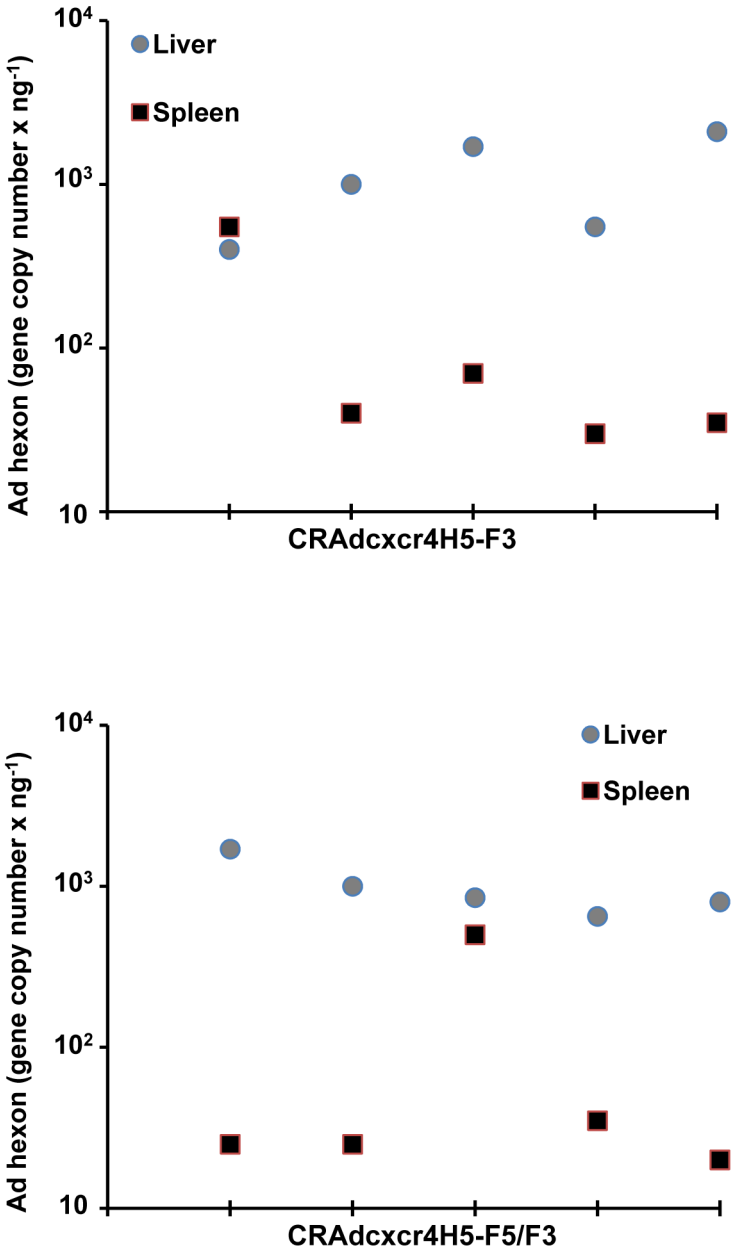

**Figure 5B**

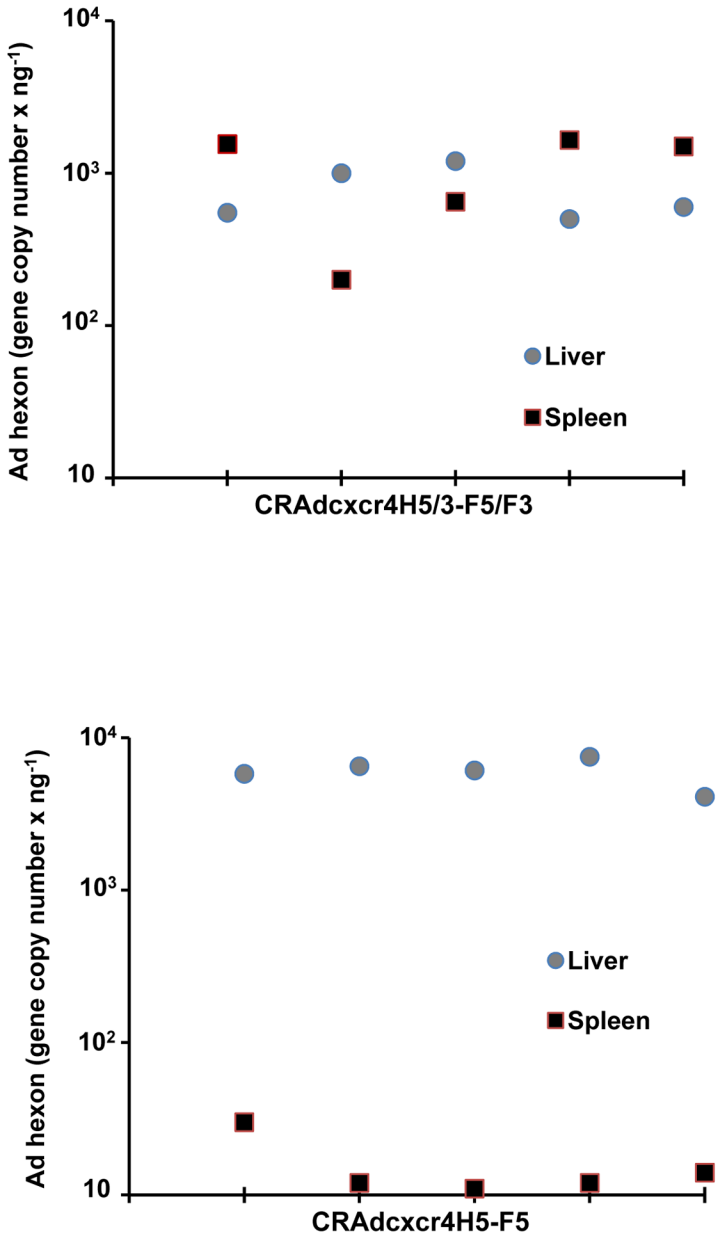

**Figure 5C**

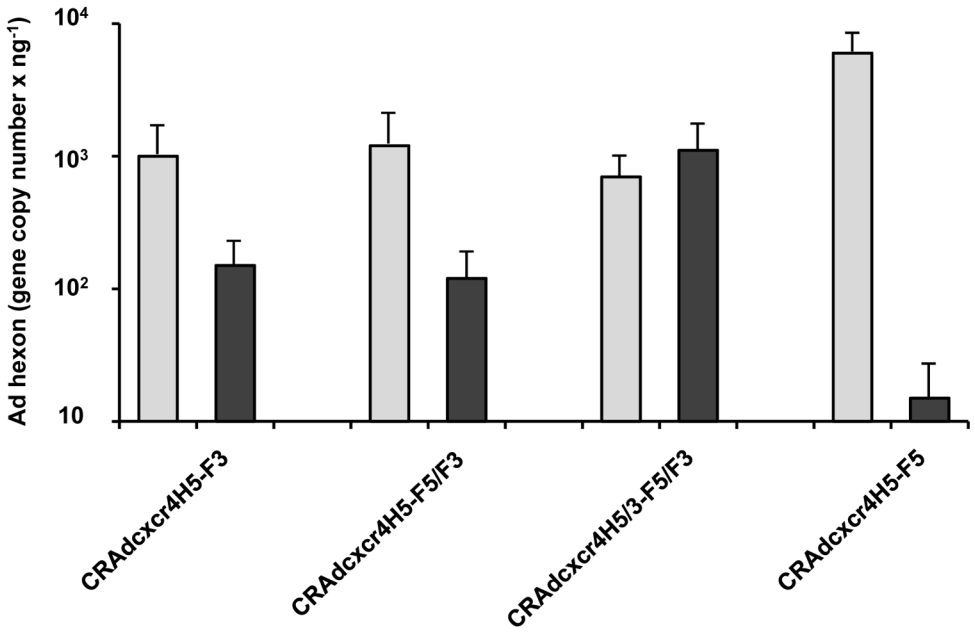

**Figure 5D**

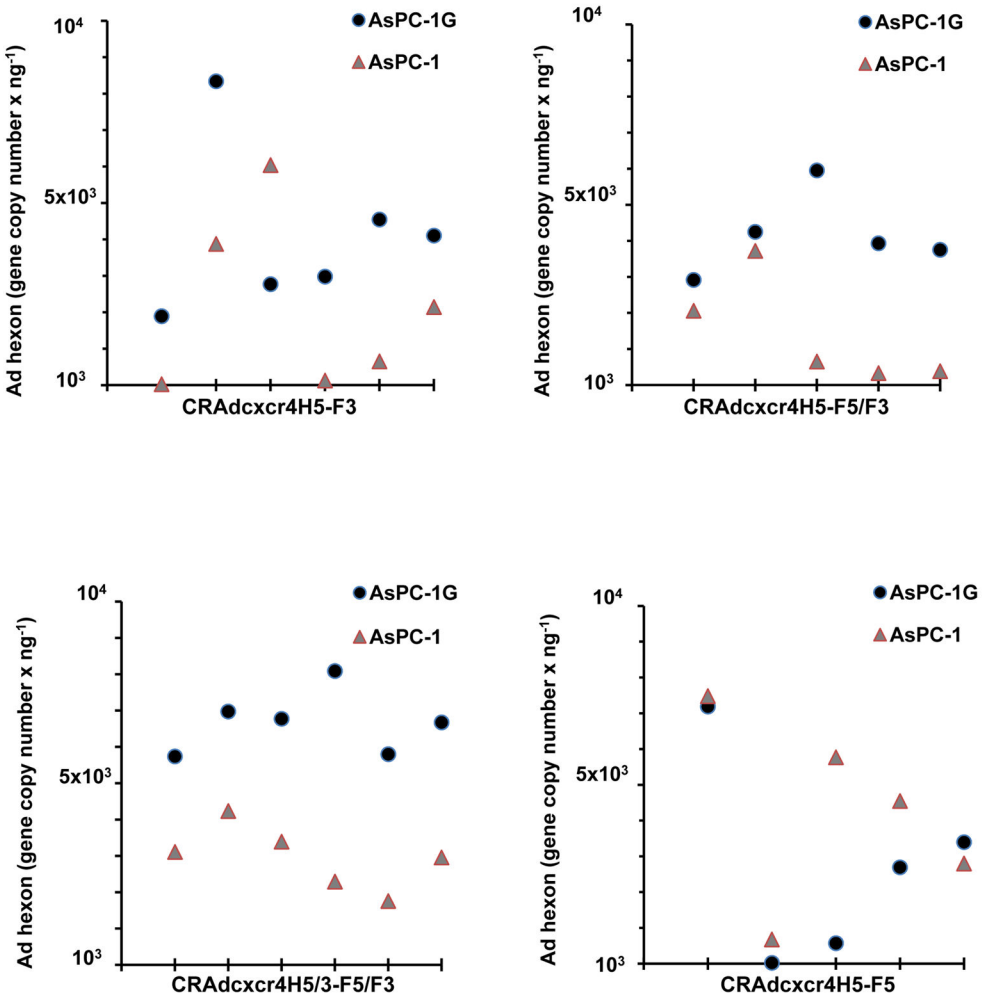

Figure 5E

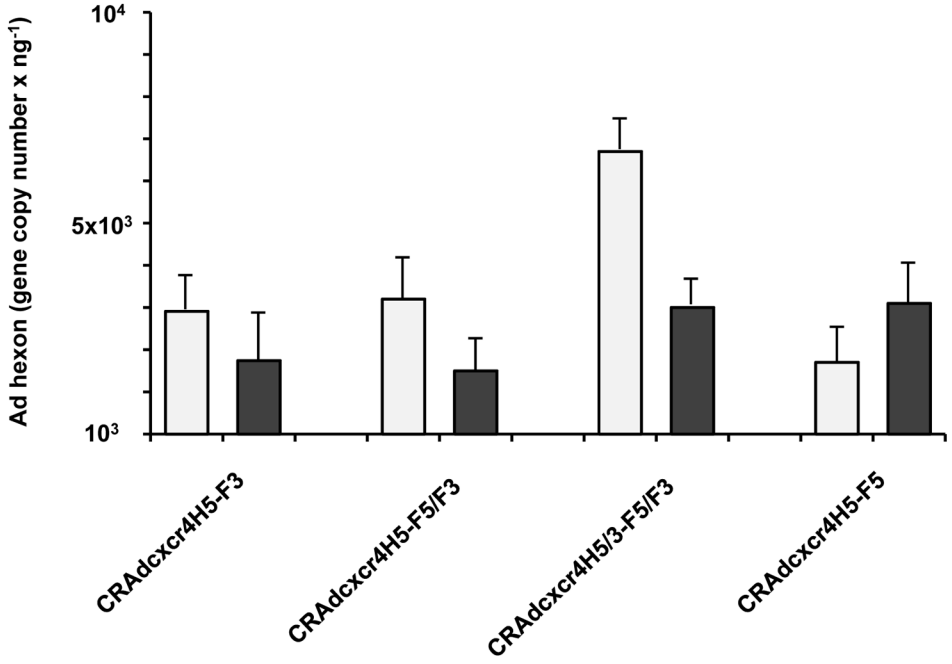


Figure 5F

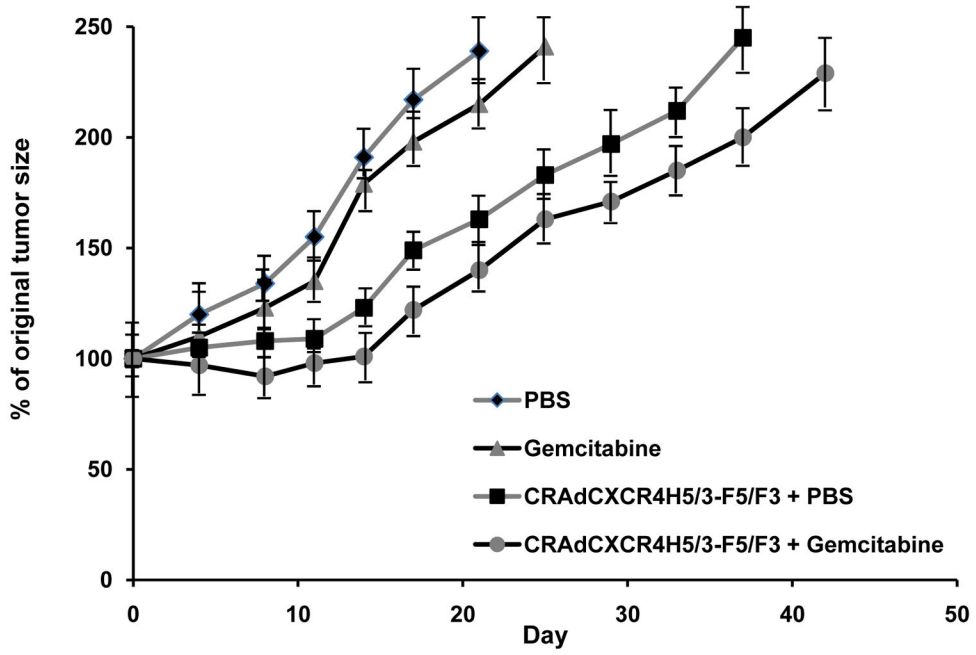


**Figure 5.**

*In vivo* characterization of CRAds. (**a**) CRAd replication in human pancreatic tumor xenografts. AsPC-1 and AsPC-1G human pancreatic tumor xenografts were injected *i.t.* with

$1 \times 10^{10}$ vp of CRAdcxcr4H5-F5 or CRAdcxcr4H5-F5/F3. Tumor tissues were collected on days 1 and 5 after injection and viral titer was measured by quantitative PCR. Presented are mean values of Ad hexon gene copy number per ng of total DNA + s.d. (**b**) Biodistribution of CRAd vector particles after systemic administration in athymic nude mice. The number of Ad hexon gene copies in liver and spleen was measured by quantitative PCR for each individual animal at 5 days following *i.v.* injection with CRAdcxcr4H5-F3, CRAdcxcr4H5-F5/F3, CRAdcxcr4H5/3-F5/F3 or CRAdcxcr4H5-F5. (**c**) The number of Ad hexon gene copies in liver (black columns) and spleen (gray columns) was measured by quantitative PCR in mice that received *i.v.* injection with CRAdcxcr4H5-F3, CRAdcxcr4H5-F5/F3, CRAdcxcr4H5/3-F5/F3 or CRAdcxcr4H5-F5. Presented are mean values of Ad hexon gene copy number per ng of total DNA + s.d. (**d**) CRAd replication in human pancreatic tumor xenografts following systemic administration. AsPC-1 and AsPC-1G cells were *s.c.* injected into the left and right flanks of athymic nude mice, respectively. Mice were injected *via* tail vein with CRAdcxcr4H5-F3, CRAdcxcr4H5-F5/F3, CRAdcxcr4H5/3-F5/F3 or CRAdcxcr4H5-F5 vectors, at 5 days after injection tumors were harvested and the number of Ad hexon gene copies was measured by quantitative PCR for each individual animal. (**e**) CRAd replication in human pancreatic AsPC-1 (black columns) and AsPC-1G (gray columns) tumor xenografts following systemic administration of CRAdcxcr4H5-F3, CRAdcxcr4H5-F5/F3, CRAdcxcr4H5/3-F5/F3 or CRAdcxcr4H5-F5. Presented are mean values of Ad hexon gene copy number per ng of total DNA + s.d. (**f**) Efficacy of combination of oncolytic virotherapy with chemotherapy in a human pancreatic tumor xenograft model. AsPC-1G cells were *s.c.* injected into the flank of athymic nude mice. *In vivo* tumor therapy was initiated on Day 0, which corresponded to 12 days post-tumor cell injection. Gemcitabine was administered *i.p.* at 100 mg/kg on Days 0, 3, 5 and 7. Animals were injected *i.v.* with $1 \times 10^{10}$ vp CRAdcxcr4H5/3-F5/F3 on Days 2 and 9. Data points represent the mean change in tumor volume relative to Day 0 for each group of animals.